



Synthesis, spectral and thermal studies of 2,2'-bipyridyl adducts of bis(N-alkyl-N-phenyldithiocarbamato)zinc(II)

Damian C. Onwudiwe^a, Peter A. Ajibade^{a,*}, B. Omondi^b

^a Department of Chemistry, University of Fort Hare, Private Bag X1314, Alice 5700, South Africa

^b Department of Chemistry, University of Johannesburg, Auckland Park Kingsway Campus, Auckland Park 2006, South Africa

ARTICLE INFO

Article history:

Received 9 October 2010

Received in revised form 17 November 2010

Accepted 17 November 2010

Available online 28 November 2010

Keywords:

Dithiocarbamate

2,2'-Bipyridyl

Adducts

Zinc(II)

Crystal structure

ABSTRACT

Three Zn(II) adducts of N-alkyl-N-phenyl dithiocarbamate with 2,2'-bipyridine have been synthesized and characterized by elemental analysis and spectroscopic techniques. The compounds are formulated as [Zn(mpdtc)₂bpy] (**1**), [Zn(epdte)₂bpy] (**2**), and [Zn(bpdtc)₂bpy] (**3**) (where m = methyl, e = ethyl, b = butyl; p = phenyl and bpy = 2,2'-bipyridine). The single crystal X-ray structures of compounds (**1**) and (**2**) are also reported. It revealed that compound (**1**) exists as a five coordinate trigonal bipyramidal structures in which one dithiocarbamate acts as a chelating ligand and the other occupying the apical position acts as a monodentate ligand, while compound (**2**) exists as six coordinate octahedral species. Each of the two compounds has four molecules in the unit cell with the uncoordinated S atom in complex **1** involved in a weak C–H...S interaction. The thermal decomposition profiles of the compounds are also reported.

© 2010 Elsevier B.V. All rights reserved.

1. Introduction

The chemistry of dithiocarbamate complexes have been extensively studied and reported for a great number of metal ions because of their striking structural features, diversified industrial applications [1,2] and biological applications [3]. The most important properties of dithiocarbamates are their strong metal-binding ability and the ease with which these complexes undergo sequential one-electron transfer reactions [4]. Group 12 metal complexes of dithiocarbamate are disposed toward a four coordinate (MS₄) geometry. They also have the tendency of forming a higher coordination number due to their large ionic size (≈2.8–2.9 Å) and the small bite angle (≈71.0–79.9 Å) of the dithiocarbamate ligands. Hence, in the ML₂ form (L = dithiocarbamate), they are coordinately unsaturated leading to the formation of compounds of higher geometry either by the addition of one or two molecules of a Lewis base or by polymerization [5,6]. In recent years, the attention has been on studying the interaction with different types of nitrogenous Lewis bases [7,8] and the fascinating structural conformations which result as the base occupies a higher coordination position. The nitrogen donor adducts of dithiocarbamate are usually highly volatile in vacuum and are of practical interest in the preparations of thin-film semiconductors [9–11] as well as electro-luminescent [12] films of transition metal sulfides. Herein, we

report the synthesis, characterization and thermal studies of bipyridyl adducts of zinc(II) dithiocarbamate.

2. Experimental

2.1. Materials and measurements

All solvents and chemicals were of analytical grade and used without further purification. Microanalyses were carried out with a Perkin-Elmer 240 elemental analyzer. The IR spectra were recorded as KBr discs on a Perkin Elmer 2000 FTIR spectrophotometer in the range 4000–370 cm⁻¹ region. ¹H and ¹³C NMR spectra were recorded on 400 and 101 MHz Bruker NMR spectrometers, respectively. Chemical shifts are given in ppm (δ scale) relative to tetramethylsilane (for ¹H and ¹³C nuclei). Thermogravimetric analysis was performed on a Perkin Elmer thermogravimetric analyzer (TGA 7) fitted with a thermal analysis controller (TAC 7/DX). A flow of N₂ was maintained with a heating rate of 10 °C/min between ambient temperature and 750 °C. Ten to 12 mg of the sample was loaded into an alumina cup and weight changes were recorded as a function of temperature. UV/visible spectra were recorded using Perkin Elmer 250 UV spectrophotometer in chloroform.

2.2. Synthesis of adducts

The precursor complexes were prepared as reported earlier [13]. The adducts were prepared by adding a 20 mL hot chloroform solution of 2,2'-bipyridine (0.40 mmol, 0.062 g) into a hot 20 mL

* Corresponding author. Tel.: +27 040 602 2055; fax: +27 040 602 2094.

E-mail address: pajibade@ufh.ac.za (P.A. Ajibade).

solution of 0.40 mmol ([Zn(mpdtc)₂], 0.172 g); ([Zn(epdtc)₂], 0.183 g) and ([Zn(bpdtc)₂], 0.205 g), respectively, in the same solvent. The resulting yellow solution was refluxed for 20 min, then concentrated to about 10 mL and filtered. The pale yellow solids which separated out from the solution, after 48 h, were filtered and dried over anhydrous calcium chloride. Single crystals suitable for X-ray analysis were obtained from slow evaporation of dichloromethane–methanol solvent mixture of [Zn(mpdtc)₂bpy] and chloroform–ethanol (3:1) solvent mixture of [Zn(epdtc)₂bpy].

[Zn(mpdtc)₂bpy]: (Yield: 0.174 g, 75%; m.p. 200–201 °C). Anal. Calc. for C₂₆H₂₄N₄S₄Zn: C, 53.28; H, 4.13; N, 9.56; S, 21.88. Found: C, 53.78; H, 4.37; N, 10.29; S, 21.97%.

[Zn(epdtc)₂bpy]: (Yield: 0.209 g, 85%; m.p. 193–194 °C). Anal. Calc. for C₂₈H₂₈N₄S₄Zn: C, 54.76; H, 4.60; N, 9.12; S, 20.88. Found: C, 54.28; H, 4.87; N, 9.53; S, 21.12%.

[Zn(bpdtc)₂bpy]: (Yield: 0.213 g, 80%; m.p. 160–162 °C). Anal. Calc. for C₂₈H₂₈N₄S₄Zn: C, 57.34; H, 5.41; N, 8.36; S, 19.13%. Found: C, 57.68; H, 5.26; N, 8.65; S 19.69%.

2.3. X-ray crystallography

A crystal of dimensions 0.12 × 0.10 × 0.03 mm⁻³ was selected for compound **1** and glued onto the tip of a glass fibre while for compound **2** a crystal of dimensions 0.38 × 0.09 × 0.03 mm⁻³ was selected. The crystal was then mounted in a stream of cold nitrogen at 100(1) K and centered in the X-ray beam by using a video camera. The crystal evaluation and data collection for the two compounds were performed on a Bruker APEXII [14] diffractometer with Mo K α (λ = 0.71073 Å) radiation and diffractometer to crystal distance of 4.00 cm. The initial cell matrix was obtained from three series of scans at different starting angles. Each series consisted of 12 frames collected at intervals of 0.5° in a 6° range about with the exposure time of 10 s per frame. The reflections were successfully indexed by an automated indexing routine built in the APEXII program suite [14]. The final cell constants were calculated from a set of 6460 strong reflections from the actual data collection. The data were collected by using the full sphere data collection routine to survey the reciprocal space to the extent of a full sphere to a resolution of 0.75 Å. A total of 7256 data were harvested by collecting 1176 frames at intervals of 0.5° scans in ω and ϕ with exposure times of 20 s per frame for compound **1** while a total of 6476 data were harvested by collecting 1792 frames at intervals of 0.5° scans in ω and ϕ with exposure times of 10 s per frame for compound **2**. These highly redundant datasets were corrected for Lorentz and polarization effects. The absorption correction was based on fitting a function to the empirical transmission surface as sampled by multiple equivalent measurements [14].

2.4. Structure solution and refinement

The systematic absences in the diffraction data were uniquely consistent for the space group *P2₁/c* for both complexes that yielded chemically reasonable and computationally stable results of refinement. The structures were solved by direct method with SIR 97 program [15] and refined by full matrix least squares with SHELXS 97 [16] provided all non-hydrogen atoms from the *E*-map. All non-H atoms were refined with anisotropic displacement parameters. Aromatic H atoms were placed in geometrically idealized positions [C–H=0.93 Å for aromatic protons and 0.96 for methyl protons (complex **1**) and C–H=0.95 Å for aromatic protons, 0.99 Å for methylene protons and 0.98 for methyl protons] and constrained to ride on their parent atoms, with $U_{\text{iso}}(\text{H}) = 1.2U_{\text{eq}}(\text{C})$. For complex **1** the deepest residual electron-density hole ($-0.33 \text{ e } \text{Å}^{-3}$) is located 0.56 Å from S(4), and the highest peak ($0.64 \text{ e } \text{Å}^{-3}$) 0.80 Å from S(3), whereas for **2** the deepest residual

electron-density hole ($-0.35 \text{ e } \text{Å}^{-3}$) is located 1.01 Å from Zn(1), and the highest peak ($0.64 \text{ e } \text{Å}^{-3}$) 0.89 Å from C(21). Crystal data and details of data collection and refinement are given in Table 1.

3. Results and discussion

3.1. X-ray crystal structure of [Zn(mpdtc)₂bpy] (**1**) and [Zn(epdtc)₂bpy] (**2**)

The two compounds [Zn(mpdtc)₂bpy] and [Zn(epdtc)₂bpy] crystallize in the monoclinic space groups *P2₁/c*. ORTEP3 [17] drawings of [Zn(mpdtc)₂bpy] and [Zn(epdtc)₂bpy] with the numbering scheme used are shown in Figs. 1 and 2 for compound **1** and **2**, respectively. Selected bond distances and angles are presented in Tables 2.

3.1.1. Crystal structure of [Zn(mpdtc)₂bpy] (**1**)

The crystal structure consists of discrete molecular species in which the metal atom is coordinated by one methyl dithiocarbamate acting as monodentate ligand another dithiocarbamate ligand, acting in a bidentate (S, S) manner; and a bipyridine acting as a bidentate ligand through the nitrogen atoms. The zinc atoms are in a distorted [ZnS₂SN₂] trigonal bipyramidal environment. The distortion of the regular trigonal bipyramidal geometry is due to the small bite angle of the two chelating ligands; dithiocarbamate and bipyridine whose S(2)–Zn(1)–S(1) and N(2)–Zn(1)–N(1) chelate angles (71.358(17)° and 75.70(6)°, respectively) deviate significantly from the expected 90°. The bond angles

Table 1
Summary of crystal data and structure refinement.

Identification code	1	2
Empirical formula	C ₂₆ H ₂₄ N ₄ S ₄ Zn	C ₂₈ H ₂₈ N ₄ S ₄ Zn
Formula weight	586.10	614.15
Temperature	100(2)	100(2)
Wavelength (Å)	0.71073	0.71073
Crystal system	Monoclinic	Monoclinic
Space group	<i>P2₁/c</i>	<i>P2₁/c</i>
<i>Unit cell dimensions</i>		
<i>a</i> (Å)	9.2157(19)	15.3418(9)
<i>b</i> (Å)	16.205(3)	9.2970(5)
<i>c</i> (Å)	17.851(4)	24.9359(12)
β (°)	105.597(9)	125.914(3)
γ (°)	90	90
Volume (Å ³)	2567.7(9)	2880.5(3)
<i>Z</i>	4	4
<i>D</i> _{calc} (Mg/m ³)	1.516	1.416
Absorption coefficient (mm ⁻¹)	1.306	1.167
<i>F</i> (0 0 0)	1208	1272
Crystal size (mm)	0.38 × 0.09 × 0.03	0.12 × 0.10 × 0.03
Theta range (°)	1.73–28.49	1.64–28.54
Index ranges	–12 ≤ <i>h</i> ≤ 12 –21 ≤ <i>k</i> ≤ 17 –23 ≤ <i>l</i> ≤ 23	–20 ≤ <i>h</i> ≤ 20 –12 ≤ <i>k</i> ≤ 12 –33 ≤ <i>l</i> ≤ 32
Reflections collected	46,454	32,564
Independent reflection	6476 [R(int) = 0.0372]	7256 [R(int) = 0.0604]
Refinement method	Full-matrix least-squares on <i>F</i> ²	Full-matrix least-squares on <i>F</i> ²
Completeness to $\theta = 28.49^\circ$	99.6	98.9
Data/restraints/parameters	6476/1/318	7256/2/336
Goodness-of-fit on <i>F</i> ²	1.053	1.008
Final <i>R</i> indices [<i>I</i> > 2 σ (<i>I</i>)]	<i>R</i> ₁ = 0.0290, <i>wR</i> ₂ = 0.0697	<i>R</i> ₁ = 0.0346, <i>wR</i> ₂ = 0.0687
<i>R</i> indices (all data)	<i>R</i> ₁ = 0.0366, <i>wR</i> ₂ = 0.0728	<i>R</i> ₁ = 0.0587, <i>wR</i> ₂ = 0.0774
Largest diff. Peak and hole e Å ⁻³	0.644 and –0.327	0.635 and –0.351

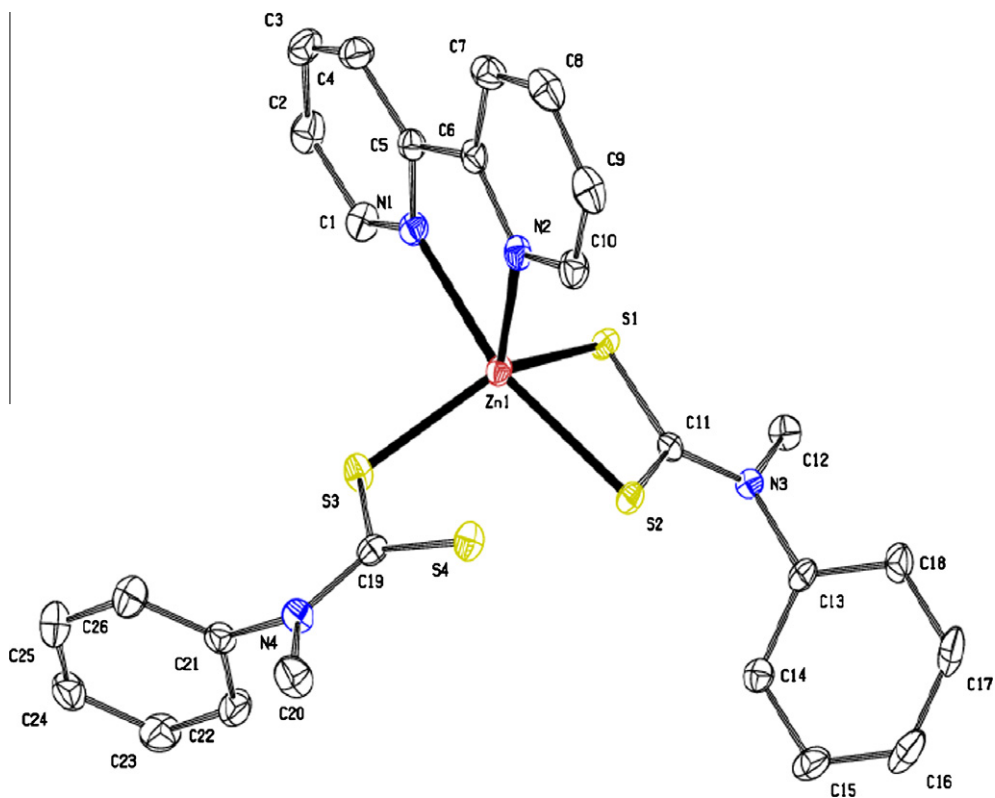


Fig. 1. ORTEP plots of $[\text{Zn}(\text{mpdtc})_2\text{bpy}]$. Hydrogen atoms have been omitted for clarity and ellipsoids are drawn at 50% probability level.

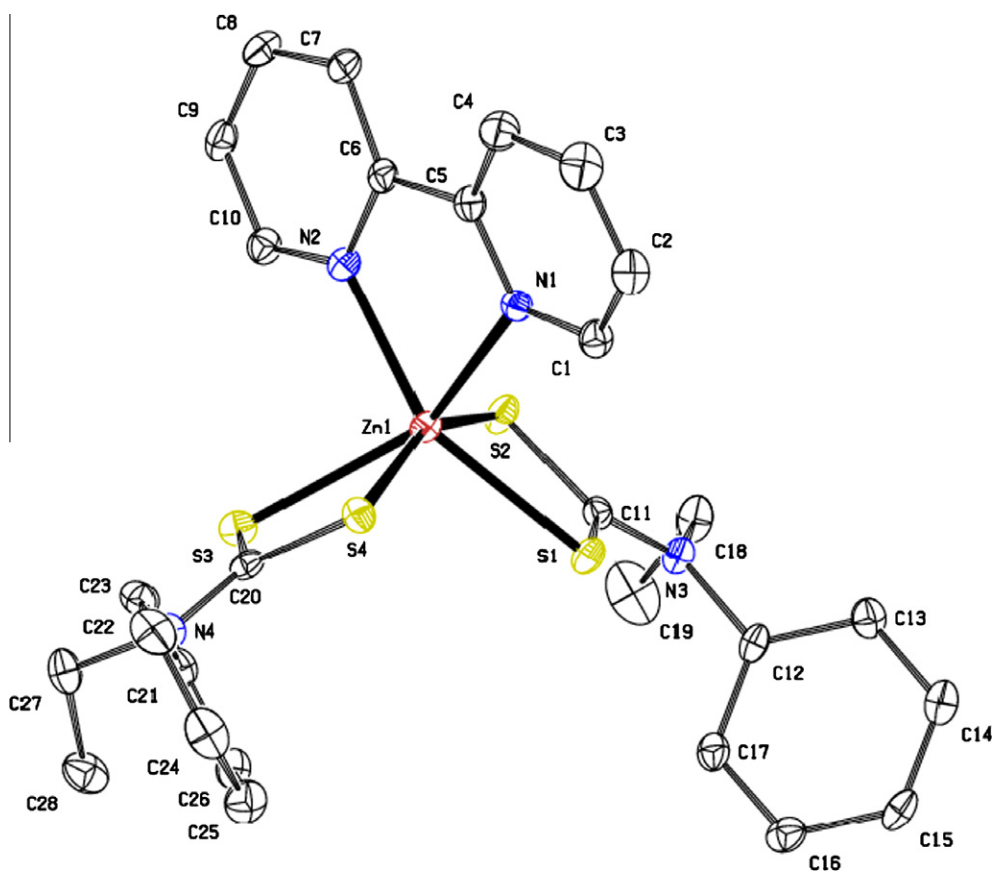


Fig. 2. ORTEP plot of $[\text{Zn}(\text{epdtc})_2\text{bpy}]$. Hydrogen atoms have been omitted for clarity and ellipsoids are drawn at 50% probability level.

Table 2
Selected bond distances (Å) and angles (°) for complexes **1** and **2**.

Distance	1	2	Angles	1	2
Zn(1)–N(1)	2.238(2)	2.235(2)	N(1)–Zn(1)–N(2)	75.70(6)	73.39(7)
Zn(1)–N(2)	2.087(2)	2.180(2)	N(1)–Zn(1)–S(1)		95.15(5)
Zn(1)–S(1)	2.480(7)	2.4486(6)	N(1)–Zn(1)–S(2)	87.71(4)	111.13(5)
Zn(1)–S(2)	2.4230(7)	2.5830(6)	N(1)–Zn(1)–S(3)	90.05(4)	144.98(5)
Zn(1)–S(3)	2.3444(6)	2.5389(6)	N(1)–Zn(1)–S(4)	160.44(4)	84.35(5)
Zn(1)–S(4)	3.427(7)	2.5226(6)	N(2)–Zn(1)–S(1)	113.58	152.38(5)
C(11)–S(1)	1.715(2)	1.717(2)	N(2)–Zn(1)–S(2)	113.58(4)	89.10(5)
C(11)–S(2)	1.721(2)	1.706(2)	N(2)–Zn(1)–S(3)	114.48(4)	91.11(5)
C(19)–S(3)	1.746(2)		N(2)–Zn(1)–S(4)	106.70(5)	109.88(5)
C(19)–S(4)	1.689(2)		S(1)–Zn(1)–S(2)		71.358(18)
C(20)–S(3)		1.717(2)	S(3)–Zn(1)–S(4)	105.87(2)	71.438(19)
C(20)–S(4)		1.713(2)	S(1)–Zn(1)–S(3)		110.82(2)
			S(1)–Zn(1)–S(4)		
			S(2)–Zn(1)–S(3)	129.62(2)	99.53(2)
			S(2)–Zn(1)–S(4)	73.439(17)	158.71(2)

for N(2)–Zn(1)–S(1) [113.58(4)°], N(2)–Zn(1)–S(1) [113.58(4)°], N(2)–Zn(1)–S(3) [114.48(4)°], N(2)–Zn(1)–S(4) [114.48(4)°] and S(3)–Zn(1)–S(4) [105.87(2)°] are significantly different from the expected 90° while N(1)–Zn(1)–S(3) [90.05(4)°] and N(1)–Zn–S(2) [87.71(4)°] are very close to the ideal value. The angle described by the equatorial positions should be close to 120°; while S(3)–Zn–S(2) [129.62(2)°] is greater than 120°, the other angles involving S(3) are less than 120°. This may be due to the steric requirement of the dithiocarbamate and bipyridine chelate but it also significantly affect the N(1)–Zn(1)–S(4) [160.44(4)°] bond angle which is far from the ideal value of 180°. The rest of the angles around the Zn atom range from 73–44(2)–129.62(2)° significantly from the ideal right angle geometry. The Zn–S bond length in [Zn(mpdtc)₂bpy]; S(3)–Zn(1) [2.3444(6)° and S(4)–Zn(1) [2.4228(6)°] are greater than the average value of tetraordinated complexes and much more shorter than those reported for hexacoordinated complexes but the values agree well with those found in other pentacoordinated complex containing similar ligands [18–20]. The Zn–N bond distances are similar in both complexes and the angle between the planes defined by the phenyl ring atoms of the bipyridyl ligand [N(1)–C(1)–C(2)–C(3)–C(4)–C(5) and N(2)–C(6)–C(7)–C(8)–C(9)–C(10)] is smaller in five coordinate complex **1** (6.5(3)°) as compared to the six coordinate complex **2** (15.9(1)°). The packing diagram of the complex (Fig. 3) consists of four molecules in the crystal lattice. The free S atom in the complex is linked through intramolecular H-bonding to the chelating S atom in a weak C–H···S interaction.

3.1.2. Crystal structure of [Zn(epdtc)₂bpy] (**2**)

The compound is monomeric with four molecules per unit cell. The zinc atom is in a distorted octahedral environment formed by four sulphur atoms from two dithiocarbamate molecules acting as

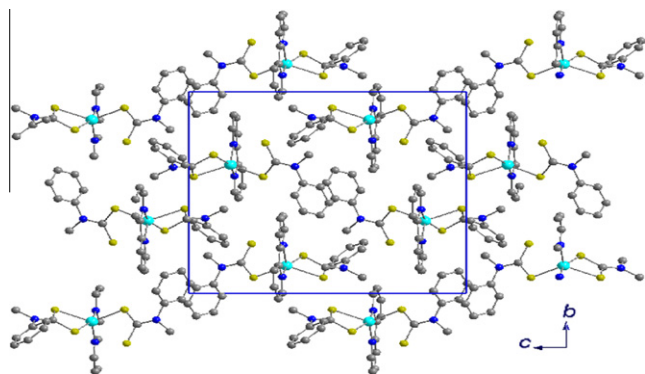


Fig. 3. Crystal packing for complex **1**.

bidentate chelating ligands, and two nitrogen atoms from the bipyridine molecule in a ZnS₄N₂ format. The Zn–S distances are S(1)–Zn(1) [2.4486(6) Å], S(2)–Zn(1) [2.5830(6) Å], S(3)–Zn(1) [2.5389(6) Å] and S(4)–Zn(1) [2.5226(6) Å]. The difference between the bond length S(1)–Zn(1), in comparison to the other, might be responsible for S(2)–Zn–(1) bond length being relatively longer than the rest. The N(2)–Zn(1)–N(1) angle of 73.39(9)° is similar to the value obtained in other bipyridine adducts of dithiocarbamate [19]. The other angles around the Zn atom are S(1)–Zn(1)–S(2) [71.358(18)°] and S(4)–Zn(1)–S(3) [71.438(19)°]. The bite angles of the chelating dithiocarbamate is less than those observed in simple dithiocarbamate complexes due to the increase in the coordination number around the zinc atom. The reduction in the bite angles might also be responsible for the changes observed in the Zn–S bond lengths. The C–S bond lengths ranges from 1.706(2) Å to 1.717(2) Å with a mean value of 1.713(2) Å, which is shorter than the 1.81 Å observed in a typical C–S single bond. Thus all the C–S bond in the complex have partial double bond character common in most dithiocarbamate compounds. The carbon nitrogen bond distances C(11)–N(3) [1.344(3) Å] and C(20)–N(4) [1.342(3) Å] confirm the presence of the partial double bond. The N(1)–Zn(1) [2.2354(18) Å] and N(2)–Zn(1) [2.1801(18) Å] distances are in the range typically observed for six coordinate complexes containing the bipyridine ligand [18–20]. The packing diagram of the complex (Fig. 4) showed that the complex has four molecules in the unit cell.

3.2. Infrared spectral studies

The IR spectra of the free ligands, the precursor complexes and their respective adducts were compared and assigned with careful comparison. The most significant difference between the compound and their corresponding precursor complexes were observed

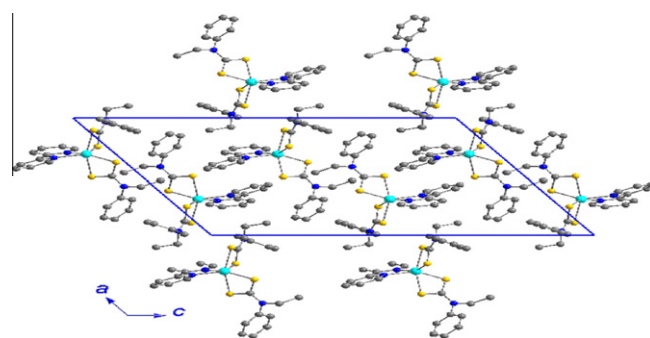


Fig. 4. Crystal packing for complex **2**.

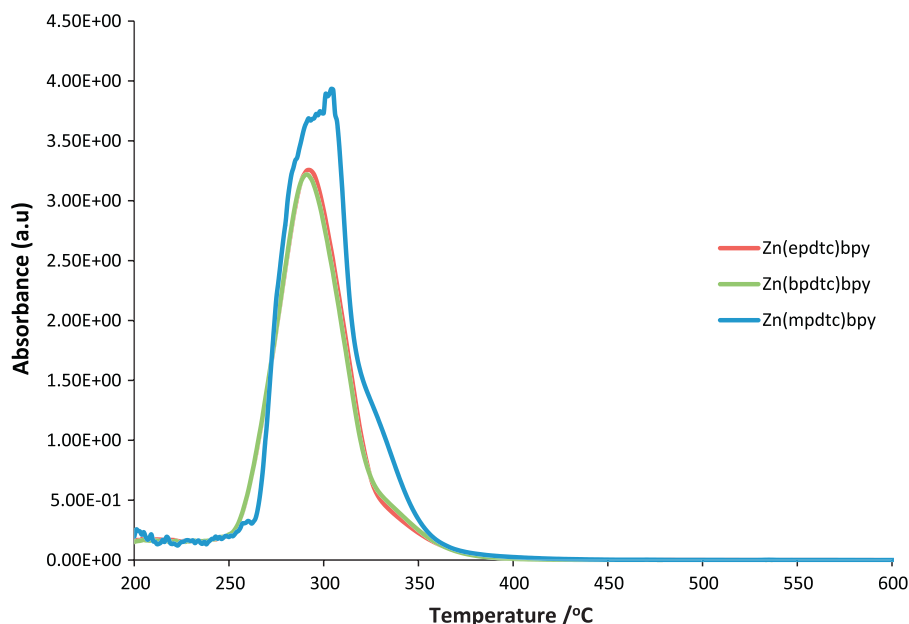


Fig. 5. Superimposed electronic spectra of [Zn(mpdtc)₂bpy], [Zn(epdtc)₂bpy] and [Zn(bpdtc)₂bpy].

in the position of the $\nu(\text{C-N})$ and $\nu(\text{C-S})$ band. The thiureide band $\nu(\text{C-N})$ which appear at 1491, 1456 and 1455 cm^{-1} in the precursor complexes is shifted to 1449, 1441, and 1440 cm^{-1} , respectively for the adducts [Zn(mpdtc)₂bpy], [Zn(epdtc)₂bpy] and [Zn(bpdtc)₂bpy]. The lowering of the $\nu(\text{C-N})$ values with respect to the parent complexes may be due to two possible reasons; one being the change in coordination geometry from tetrahedral (four coordinate in the starting materials?) to octahedral (six coordinate) [21], which affect the degree of interaction between the dithiocarbamate ligands and the zinc ion leading to a reduction in the vibrational frequency. The second reason could be the transfer of electrons from the nitrogen of the bipyridine ligand to the zinc ion enriching the metal electron density upon the adduct formation [22]. The lengthening of alkyl chain has been found to be accompanied by a decrease in the vibrational frequency of $\nu(\text{C-N})$ [23] and this accounts for the lower vibrational frequency observed in the $\nu(\text{C-N})$ of adduct which contains the butyl substituent. The $\nu(\text{C-S-S})$ mode is usually expected around $1000 \pm 70 \text{ cm}^{-1}$ region. Based on Bonati and Ugo criterion [24], the number of bands observed in this region could be used to determine the binding mode of the dithiocarbamate ligand. While the spectra of [Zn(epdtc)₂bpy] and [Zn(bpdtc)₂bpy] show a single peak at 969 and 965 cm^{-1} , respectively, which is strongly indicative of a bidentate coordination of the dithiocarbamate moiety [25], the spectra of compound [Zn(mpdtc)₂bpy] displays a different feature in this region. A single sharp band appeared at 970 cm^{-1} which is attributed to $\nu(\text{C-S})$ stretching vibration of a symmetrical bound dithiocarbamate ligand. In addition, two other peaks appeared at 1017 and 1002 cm^{-1} showing the presence of unsymmetrically bonded dithiocarbamate indicating that in the adduct, [Zn(mpdtc)₂bpy], both the monodentate and bidentately coordinated dithiocarbamate are present in the molecular structure (see Fig. 1). A further confirmation of this was obtained from the single crystal X-ray structure of the complex.

3.3. NMR spectral studies

The ¹H NMR spectra of all the compounds show signals for the hydrogen of the methyl, integrated as six protons, in three distinctly separate positions, at $\delta = 3.78$ (6H, s), 1.30 (6H, t) and 0.93

(6H, t). This reflects the reduction in the deshielding effect of the electronegative *N*-atom as the distance between the nitrogen and the carbon bearing the protons increases. Both [Zn(epdtc)₂bpy] and [Zn(bpdtc)₂bpy] show signals at $\delta = 3.82$ (4H, q) and 4.17 (4H, t) ppm, respectively, which correspond to the $-\text{CH}_2$ protons on a highly deshielding atom (Nitrogen). The resonance peaks for the protons in the alkyl group of dithiocarbamates have been compared with that of the complex. The downfield shifts observed in the complexes are attributed to the lowered electron density. In the complexes, the $-\text{NCS}_2$ moiety is neutral, while it is anionic in the free dithiocarbamic ligands [26]. Peaks showing as four hydrogen triplet at $\delta = 1.37$ and 1.73 ppm for [Zn(bpdtc)₂bpy] are ascribed to the methylene protons of the butyl group. The phenyl ring protons appear in the range $\delta = 7.29$ –7.44 ppm in all the compounds. This indicates a weak deshielding and could be attributed to the shift of electron density towards the nitrogen of the NRR' (R = alkyl; R' = phenyl) thereby enhancing the electron density on the sulphur via the thioureide π -system [9]. The peaks around $\sigma = 7.91$, 8.25, 8.27, and 9.06 ppm are due to the ring protons of 2,2'-bipyridine. The peak at $\delta = 9.06$ ppm is clearly the protons adjacent to the coordinated nitrogen. The shift downfield observed for the protons of the 2,2'-bipyridine compared to the free 2,2'-bipyridine results from the reduced electron density as a result of the loss of lone pair of electron into the zinc atom upon coordination, and the proximity to the $-\text{NCS}_2$.

The ¹³C NMR spectra of the three compounds show five signals in the region $\sigma = 121.00$ –129.00 ppm which correspond to the aromatic carbons from the phenyl substituent of the dithiocarbamate ligand, and also between $\sigma = 137.00$ –149.00 ppm that are ascribed to 2,2'-bipyridine carbons. The signals for the carbon of the methylene bound to nitrogen in the dithiocarbamate are observed between 47.48 and 59.28 ppm. The highest downfield shift observed in [Zn(bpdtc)₂bpy] may be due to the high inductive effect of the butyl substituent compared to the ethyl and methyl group. The resonance peak for the β - and γ -methylene carbons of the butyl group appeared at 29.70 and 20.31 ppm, respectively. All three compounds show signals around 208–209 ppm, with reduced intensity typical of quaternary carbon, that correspond to the carbon of the $-\text{NCS}_2$. The down field shift of the NCS_2 moiety compared to the parent complexes, observed between 206.00 and

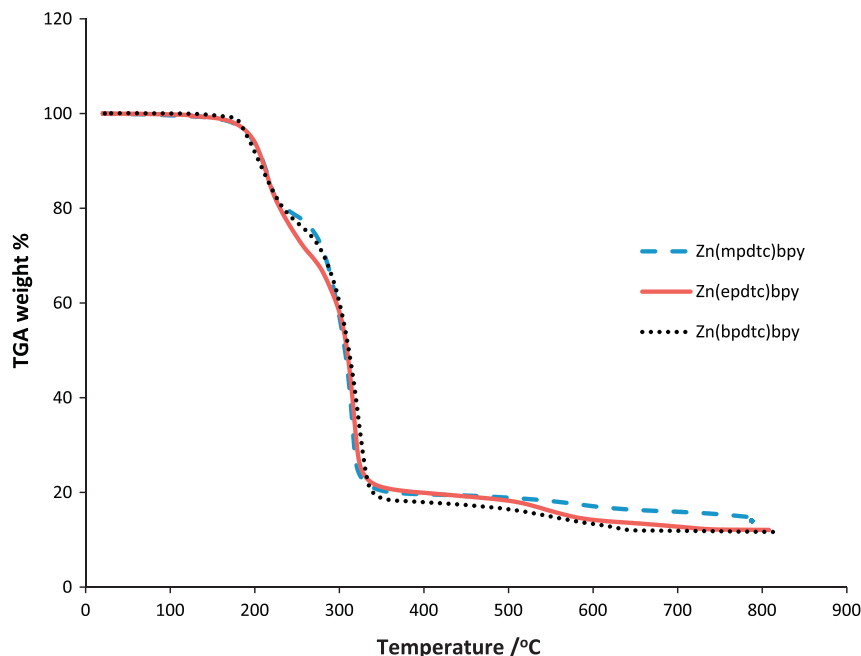


Fig. 6. Thermograms of $[\text{Zn}(\text{mpdtc})_2\text{bpy}]$, $[\text{Zn}(\text{epdtc})_2\text{bpy}]$ and $[\text{Zn}(\text{bpdtc})_2\text{bpy}]$.

Table 3

Temperature values for decomposition along with corresponding weight loss values and product obtained.

Compounds	Decomposition range (°C)	Peak temperature (°C)	Weight loss (%)	Product obtained	Mass changes	
					Calc.	Found
$[\text{Zn}(\text{mpdtc})_2\text{bpy}]$	150–235	211	28	$\text{Zn}(\text{mpdtc})$	2.64	2.11
	240–360	314	79	$\text{Zn}(\text{NCS})_2$	3.10	3.45
	531–621	580	84	ZnS	1.67	1.68
$[\text{Zn}(\text{epdtc})_2\text{bpy}]$	142–244	213	24	$\text{Zn}(\text{epdtc})$	2.22	3.02
	256–346	316	72	$\text{Zn}(\text{NCS})_2$	3.63	3.29
	496–587	527	85	ZnS	1.95	1.93
$[\text{Zn}(\text{bpdtc})_2\text{bpy}]$	160–241	190	21	$\text{Zn}(\text{bpdtc})$	3.01	2.79
	242–360	319	76	$\text{Zn}(\text{NCS})_2$	3.50	3.68
	567–642	617	84	ZnS	1.88	1.57

207.00 ppm, may be ascribed to an increase of π -bond character or delocalization of electron along the C–N bond which is enhanced by the unshared electron pair in the nitrogen atom [27]. The electron donating effect by the alkyl substituents and the bidentate nature of the dithiocarbamate ligand might also have a contributory role [28].

3.4. Electronic spectra of the complexes

The UV–Vis spectra of the three complexes are shown in Fig. 5. The UV spectra of dithiocarbamate complexes are usually characterized by three absorption bands due to chromospheres group NCS_2 and are attributed to $\pi \rightarrow \pi^*$ transition of NCS and SCS moiety; and $n \rightarrow \pi^*$ transition involving the transition of an electron of the lone pair on the sulphur atom to an antibonding π -orbital [29]. In the present complexes, these bands are overlapped by an intense band between 294 and 298 cm^{-1} due to the $\pi \rightarrow \pi^*$ transition of the phenyl ring [30]. No splitting of band is observed in $[\text{Zn}(\text{epdtc})_2\text{bpy}]$ and $[\text{Zn}(\text{bpdtc})_2\text{bpy}]$ while $[\text{Zn}(\text{mpdtc})_2\text{bpy}]$ undergoes a peak splitting which indicates the non-equivalence of the C–S bond [31]. There is no evidence of any d–d transition over the visible region indicating d^{10} electronic configuration of the d^{12} metals.

3.5. Thermogravimetric analysis

The thermogravimetric analysis (TGA) of the samples was performed under a nitrogen atmosphere with a heating rate of $10^\circ\text{C min}^{-1}$, as depicted in Fig. 6. Temperature values for decomposition along with corresponding weight loss values and product obtained are presented in Table 3. The three complexes display similar thermogram which indicates that their mechanism of decomposition is the same when heated. The decomposition started with a weight loss of 26.4%, 24.8% and 22.4% in a clearly marked step for $[\text{Zn}(\text{mpdtc})_2\text{bpy}]$, $[\text{Zn}(\text{epdtc})_2\text{bpy}]$ and $[\text{Zn}(\text{bpdtc})_2\text{bpy}]$, respectively. This corresponds to the loss of the 2,2'-bipyridine fragment (Calc. 26.64%, 25.4% and 23.2%). The peak temperature of 2,2'-bipyridine expulsion decreased from $[\text{Zn}(\text{epdtc})_2\text{bpy}]$ to $[\text{Zn}(\text{bpdtc})_2\text{bpy}]$ (213 °C and 190 °C, respectively) indicating a reduction in Zn–N (of the bipyridine) bond, and a manifestation of the inductive effect of the alkyl substituents bonded to the sp^2 -hybridized nitrogen atom [32]. The increase in the inductive effect of alkyl substituents in the series CH_3 , C_2H_5 and C_4H_9 is expected to result in the progressive displacement of electron density in the $\text{R}_2\text{N}-\text{C}(\text{S})\text{S}$ -moiety from the nitrogen atom toward the zinc. The high electron density on the zinc atom of the compound with high alkyl group reduces the interaction of the zinc atom with the lone pairs of electron from the nitrogen,

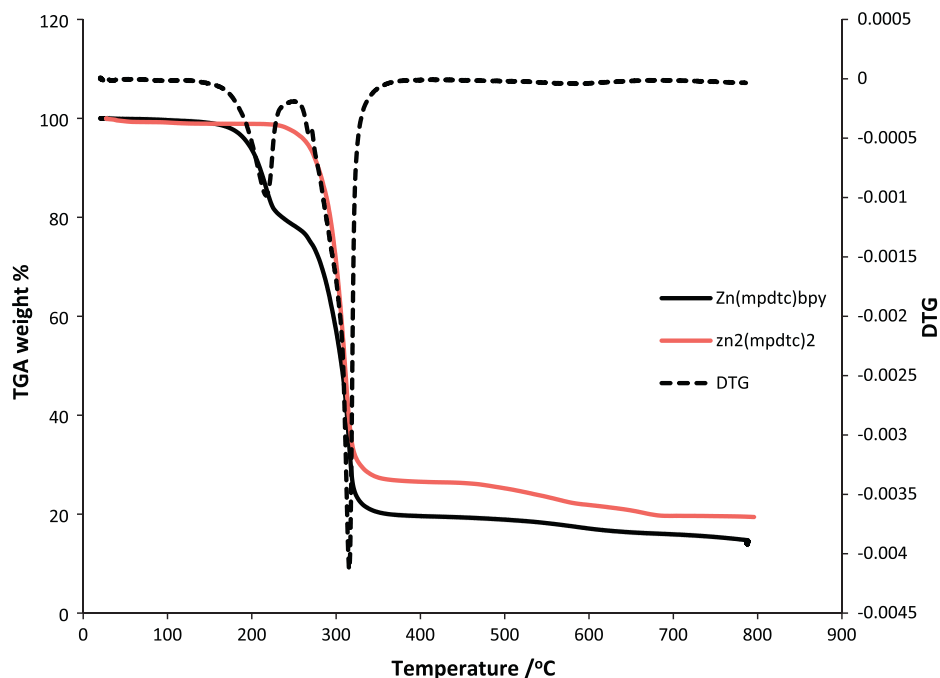


Fig. 7. Superimposed TG/DTG curves of $[Zn(mpdtc)_2bpy]$ and the TG curve of the precursor complex $[Zn_2(mpdtc)_2]$.

hence extending the bond length. The lower peak temperature observed in $[Zn(mpdtc)_2bpy]$ compared to $[Zn(epdtc)_2bpy]$ may be due to the monodentate binding mode of one of the dithiocarbamates in the former. The loss of 2,2'-bipyridine was followed immediately with a huge weight loss caused by the decay of the dithiocarbamate (72–76%), leading to the formation of $Zn(NCS)_2$ in the temperature range of approximately 240–360 °C. Further increase in temperature results in the decomposition of $Zn(NCS)_2$ to ZnS. This is similar to the observations made in the decomposition of group 12 dithiocarbamate adduct with nitrogenous bases [33]. To compare the thermal stability of the precursor complexes with

their respective adducts, the thermogram of each adduct was superimposed with its respective precursor complex (Figs. 7–9). A critical look shows that there is a shift in the thermal destruction range of the dithiocarbamate moiety toward lower temperature for the adducts compared to the parent complexes. This observation has been explained as the formation of unstable mononuclear complexes $[Zn(S_2CNRR')_2]$ $\{R = CH_3, C_2H_5, C_4H_9; R' = C_6H_5\}$ via the detachment of the N-donor base by the adducts [34]. The precursor complexes originally exist in their binuclear form [13,35,36]. EPR studies have been used for similar compounds to show the formation of such mononuclear complexes upon desorption of

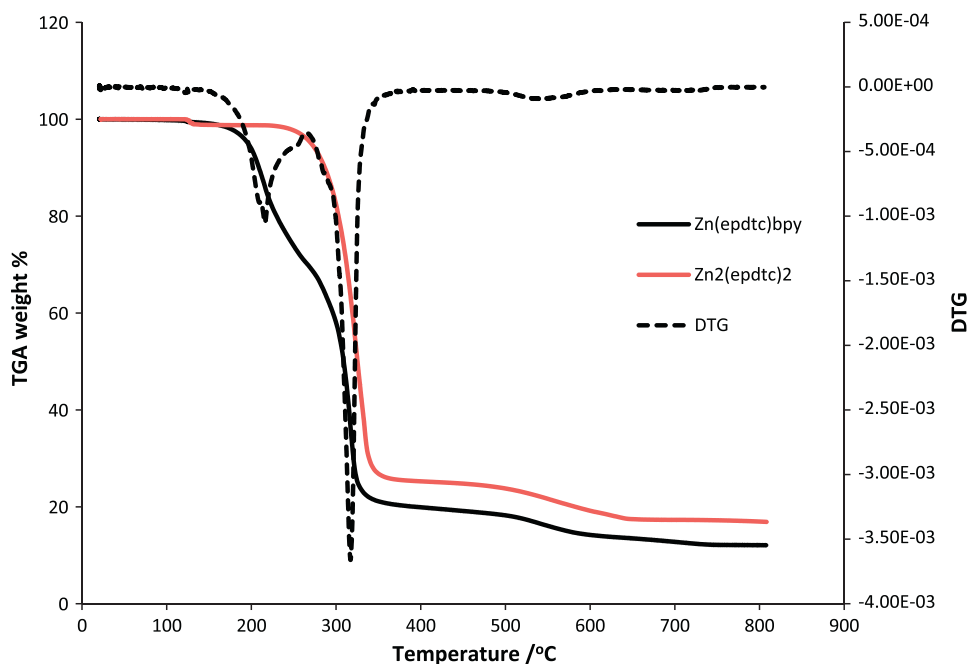


Fig. 8. Superimposed TG/DTG curves of $[Zn(epdtc)_2bpy]$ and the TG curve of the precursor complex $[Zn_2(epdtc)_2]$.

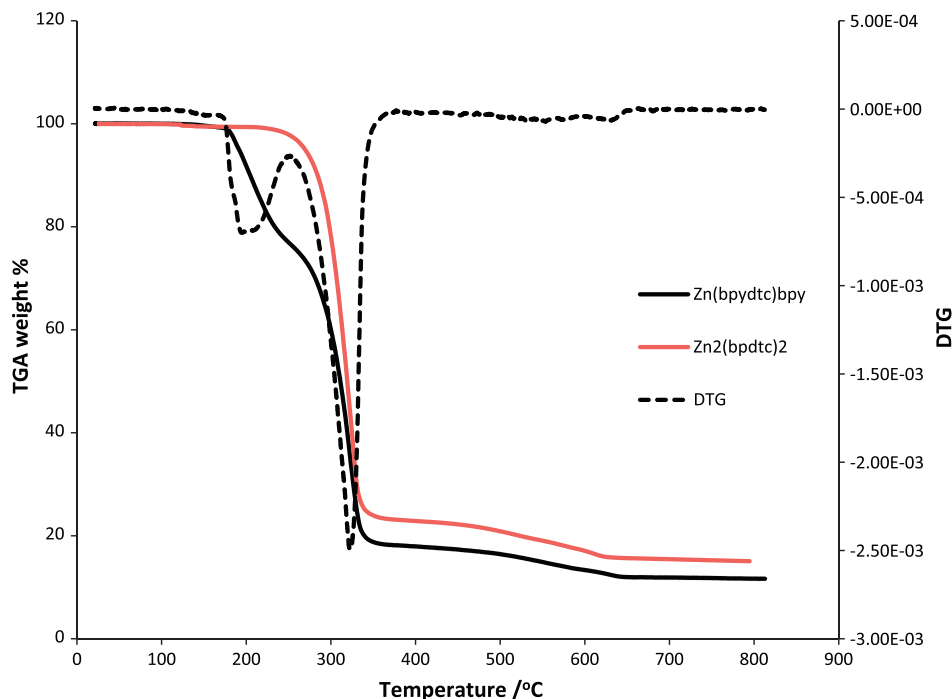


Fig. 9. Superimposed TG/DTG curves of $[Zn(bpdtc)_2bpy]$ and the TG curve of the precursor complex $[Zn_2(bpdtc)_2]$.

N-donor bases from adducts [37,38]. The absence of any plateau between the detachment of the 2,2'-bipyridine and the decomposition of the dithiocarbamate moiety further emphasizes the instability of the zinc dithiocarbamate complexes in the mononuclear state at room temperature.

4. Conclusions

Three bipyridine adduct of Zn(II) alkyl, phenyl dithiocarbamate formulated as $[Zn(mpdtc)_2bpy]$ (**1**), $[Zn(epdtc)_2bpy]$ (**2**), and $[Zn(bpdtc)_2bpy]$ (**3**) have been synthesized and characterized. Single crystal X-ray structures of two of the adducts showed that compound **1**, $[Zn(mpdtc)_2bpy]$ consist of a discrete molecular species in which the metal atom is coordinated by one methyl dithiocarbamate acting as a monodentate ligand and the other dithiocarbamate ligand acts as bidentate ligand. The bipyridine also coordinates as a bidentate ligand through the nitrogen atom resulting in severely distorted trigonal pyramidal geometry around the zinc atom defines by the atom $Zn-S_2-S-N_2$. Compound **2** has the zinc atom in a distorted octahedral environment formed by four sulphur atoms from two chelating dithiocarbamate ligands and two nitrogen atoms from the bipyridine molecule in a ZnS_4N_2 format. The thermal decomposition profiles of the complexes are also reported.

Supplementary data

CCDC 793020 and 793019 contain the supplementary crystallographic data for this paper. These data can be obtained free of charge via <http://www.ccdc.cam.ac.uk/conts/retrieving.html>, or from the Cambridge Crystallographic Data Centre, 12 Union Road, Cambridge, CB2 1EZ, UK; fax: +44 1223 336 033 or email: deposit@ccdc.cam.ac.uk.

Acknowledgements

The authors gratefully acknowledge the financial support of GMRDC, University of Fort Hare, South Africa.

References

- [1] J. Nieuwenhuizen, A.W. Ehless, J.G. Haashoot, S.R. Janse, J. Reedijk, J. Baerends, *J. Am. Chem. Soc.* 121 (1999) 163.
- [2] G.D. Thorn, R.A. Ludwig, *The Dithiocarbamates and Related Compounds*, Elsevier, New York, 1962 (Chapters 1, 3, 4).
- [3] J.S. Casas, A. Sanchez, J. Bravo, S. Garcia-Fontan, E.E. Castellano, M.M. Jones, *Inorg. Chim. Acta* 158 (1989) 119.
- [4] M. Lieder, *Electrochim. Acta* 49 (2004) 1813.
- [5] S. Thirumaran, K. Ramalingam, G. Bocelli, A. Cantoni, *Polyhedron* 19 (2000) 1279.
- [6] S. Thirumaran, K. Ramalingam, G. Bocelli, A. Cantoni, *Polyhedron* 18 (1999) 925.
- [7] G. Marimuthu, K. Ramalingam, C. Rizzoli, *Polyhedron* 29 (2010) 1555.
- [8] M. Azad Malik, M. Motevali, P. O'Brien, *Polyhedron* 18 (1999) 1259.
- [9] P.V. Subha, P. Valarmathi, N. Srinivasan, S. Thirumaran, K. Saminathan, *Polyhedron* 29 (2010) 1078.
- [10] M. Chunggaze, M.A. Malik, P. O'Brien, *Adv. Mater. Opt. Electr.* 7 (1997) 311.
- [11] P. O'Brien, D.J. Otway, J.R. Walsh, *Thin Solid Films* 315 (1998) 57.
- [12] V.G. Bessergenev, V.I. Belyi, A.A. Rastorgner, E.N. Ivanova, Y.A. Kovalerskaya, S.V. Larinov, S.M. Zemskova, V.N. Kirichenko, V.A. Nadolinniy, S.A. Gromilov, *Thin Solid Films* 279 (1996) 135.
- [13] D.C. Onwudiwe, P.A. Ajibade, *Polyhedron* 29 (2010) 1431.
- [14] Bruker-AXS, APEX2, SADABS, and SAINT Software Reference Manuals, Bruker-AXS, Madison, Wisconsin, USA, 2009.
- [15] SIR97 A. Altomare, M.C. Burla, M. Camalli, G.L. Casciarano, C. Giacovazzo, A. Guagliardi, A.G.G. Moliterni, G. Polidori, R. Spagna, *J. Appl. Cryst.* 32 (1999) 115.
- [16] SHELX [includes SHELXS86, SHELXS97, SHELXL97, CIFTAB (and SHELXA?)] G.M. Sheldrick, *Acta Cryst. A* A64 (2008) 112.
- [17] ORTEP3 for Windows L.J. Farrugia, *J. Appl. Crystallogr.* 30 (1997) 565.
- [18] M.L. Godino-Salido, M.D. Gutierrez-Valero, R. Lopez Garzon, *Inorg. Chim. Acta* 221 (1994) 177.
- [19] A. Rodriguez, A. Sousa-Pedares, J.A. Garcia-Vazquez, J. Romero, *Polyhedron* 28 (2009) 2240.
- [20] A. Sousa Pedrares, J. Romero, J.A. Garcia-Vasquez, M.L. Duran, I. Casanova, A. Sousa, *Dalton Trans.* (2003) 1379.
- [21] A.M.A. Hassan, E.M. Soliman, A.M.El. Roudi, *Polyhedron* 8 (1989) 925.
- [22] F. Jian, Z. Wang, Z. Bai, X. You, H. Fun, K. Chinnakali, I.A. Razak, *Polyhedron* 18 (1999) 151.
- [23] A. Manohar, V. Venkatachalam, K. Ramalingam, S. Thirumaran, G. Bocelli, A. Cantoni, *J. Chem. Cryst.* 28 (1998) 861.
- [24] F. Bonati, R. Ugo, *J. Org. Met. Chem.* 10 (1967) 57.
- [25] K. Nakamoto, *Infrared and Raman Spectra of Inorganic and Coordination Compounds*, fifth ed., John Wiley & Sons, New York, 1997. p. 207.
- [26] L. Ronconi, L. Giovagnini, C. Marzano, F. Bett'io, R. Graziani, G. Pilloni, D. Fregona, *Inorg. Chem.* 44 (2005) 1867.
- [27] R. Nomura, A. Takabe, H. Matsuda, *Polyhedron* 6 (1987) 411.
- [28] I. Raya, I. Baba, B.M. Yamin, *Mal. J. Anal. Sci.* 10 (2006) 93.

- [29] D. Zhu, R. Zhang, C. Ma, H. Yin, *Indian J. Chem.* 41a (2002) 1034.
- [30] C. Su, N. Tang, M. Tan, X. Gan, L. Cai, *Synth. React. Inorg. Met. – Org. Chem.* 27 (2) (1997) 291–300.
- [31] Weiguang Zhang, Yun Zhong, Minyu Tan, Ning Tang, Kaibei Yu, *Molecules* 8 (2003) 411–417.
- [32] A.V. Ivanov, O.N. Antzutkin, in: Jacek Klinowski (Ed.), *New Techniques in Solid State NMR*, 2005, p. 285.
- [33] B.A. Prakasam, K. Ramalingam, G. Bocelli, A. Cantoni, *Phosphorus, Sulfur, Silicon* 184 (2009) 2020.
- [34] A.V. Ivanov, V.I. Palazhchenko, S.A. Leskova, M.A. Mel'nikova, *Russ. J. Inorg. Chem.* 50 (2005) 1014.
- [35] I. Baba, L.H. Lee, Y. Farina, A.H. Othman, A.R. Ibrahim, A. Usman, H.-K. Fun, S.W. Ng, *Acta Cryst. E* 58 (2002) m744.
- [36] R.A. Gossage, A. Jenkins, *Acta Chim. Slov.* 56 (2009) 329.
- [37] A.V. Ivanov, P.M. Solozhenkin, V.B. Klyashtornyi, *Dokl. Akad. Nauk SSSR* 319 (1991) 403.
- [38] A.V. Ivanov, V.B. Klyashtornyi, *Zh. Neorg. Khim.* 37 (1992) 1597.